Curr Radiol Rep (2015) 3:42
DOI 10.1007/s40134-015-0124-x

Imaging Assessment of Infertile Couples: Why and When

Jeffrey Dee Olpin[1] · **Anne Kennedy**[1]

Published online: 22 September 2015

Abstract Infertility is defined as failure to achieve pregnancy during 1 year of unprotected intercourse. The clinical evaluation of infertility has become increasingly sophisticated over the past several decades. Significant advancements in reproductive medicine yield much higher fertility rates among couples with infertility issues. The evaluation of an infertile couple demands a systematic approach in order to pinpoint a specific infertility disorder. Imaging plays a fundamental role in the evaluation of the infertile couple. Clinicians and radiologists involved in reproductive medicine must have a fundamental understanding of the strengths and weaknesses of various imaging modalities in order to be effective members of the reproductive healthcare community. In particular, knowing why a particular imaging modality is employed for a suspected infertility disorder and knowing when a particular imaging study should be performed is essential in the assessment of the infertile couple.

Keywords Infertility · Fallopian tube · Uterus · Endometrium · Adenomyosis · Endometriosis

Introduction

Infertility is a worldwide problem that accounts for a steadily increasing monetary expenditure in the United States. The number of assisted reproduction procedures increased by 92 % between 1996 and 2004 [1].

Infertility is defined as the inability to conceive after 1 year of unprotected intercourse [2]. The evaluation of an infertile couple is a complex, multifactorial process that requires comprehensive evaluation of both partners. Certain causes in either gender may be suggested by a thorough history and physical examination with appropriate laboratory testing. However, many conditions can only be reliably diagnosed through the employment of imaging studies, including fluoroscopy, ultrasound (US), computed tomography (CT), and magnetic resonance (MR) imaging. Accordingly, the use of imaging for the assessment of infertile couples is likewise on the rise. Clinical radiologists involved in infertility imaging must be able to aid reproductive specialists in the optimal utilization of various imaging modalities employed in the assessment of the infertile couple.

Female Infertility

There are roughly 7.4 million women or 12 % of the female population of reproductive age in the United States that suffer from infertility according to the 2002 National Survey of Family Growth [3]. The multiple causes of female infertility may involve the fallopian tubes, uterus, cervix, peritoneal cavity, and ovaries.

This article is part of the Topical Collection on *Urogenital Imaging*.

✉ Jeffrey Dee Olpin
jeffrey.olpin@hsc.utah.edu

Anne Kennedy
anne.kennedy@hsc.utah.edu

[1] University of Utah Health Sciences Center, 30 North 1900 East #1A071, Salt Lake City, UT 84132, USA

Disorders of the Fallopian Tube

Fallopian tube occlusion is the most common cause of female infertility, accounting for 30–40 % of cases in the United States [4, 5]. Fallopian tube disorders can result in impaired transport of the mature ovum from the ovary to the uterine cavity during the process of conception. A conventional hysterosalpingogram (HSG) is generally regarded as the most appropriate initial imaging study in the workup of an infertile female. An HSG can readily assess tubal patency, tubal irregularity, and peritubal disease [6]. Extra-tubal disorders of the female reproductive system may be inferred on a conventional HSG, but frequently require additional imaging studies for confirmation (Chart 1).

Common etiologies of tubal occlusion include tubal spasm, infection, and prior surgery [6]. Tubal spasm generally occurs in the proximal or interstitial portion of the fallopian tube, is generally transient, and often resolves with delayed imaging [7]. Prone imaging at HSG may also alleviate tubal spasm [8].

The most common cause of tubal occlusion is prior pelvic inflammatory disease (PID), usually the result of sexually transmitted infection from *Chlamydia trachomatis* or *Neisseria gonorrhea* [9]. Less common etiologies of tubal occlusion include granulomatous salpingitis from prior disseminated tuberculosis, intraluminal endometriosis, parasitic infection, and congenital atresia of the fallopian tubes [7]. Imaging findings of tubal occlusion include lack of free contrast spillage into the peritoneal cavity (Fig. 1). Tubal dilatation or hydrosalpinx is commonly seen in the setting of distal tubal occlusion, usually the result of pelvic inflammatory disease.

Peritubal adhesions can result in infertility. The etiology of peritubal adhesions includes prior pelvic surgery, endometriosis, and PID [7]. The condition is readily diagnosed by peritubal pooling or entrapment of contrast surrounding the ampullary portion of the fallopian tube with lack of free intraperitoneal contrast spillage (Fig. 2).

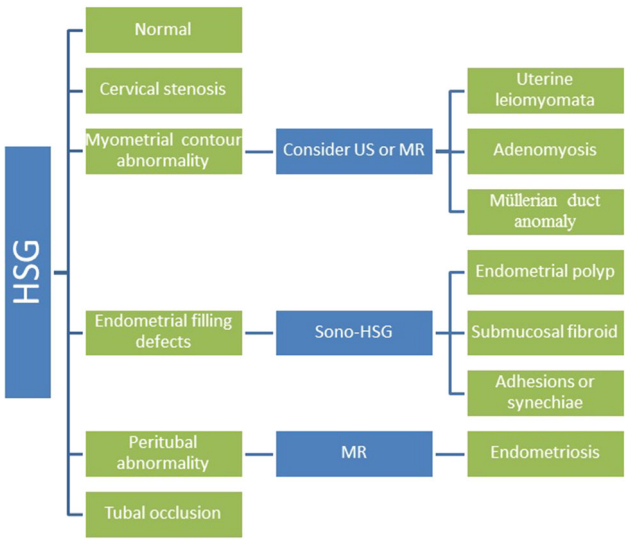

Chart 1 Algorithm for the imaging workup of female infertility

Disorders of the Uterus

Endometrial Disorders

Disorders of the endometrium may be detected on conventional HSG as intrauterine filling defects. However,

Fig. 1 Tubal occlusion. Hysterosalpingogram shows occlusion of the proximal left fallopian tube (*arrow*). There is free spillage of contrast from the right fallopian tube

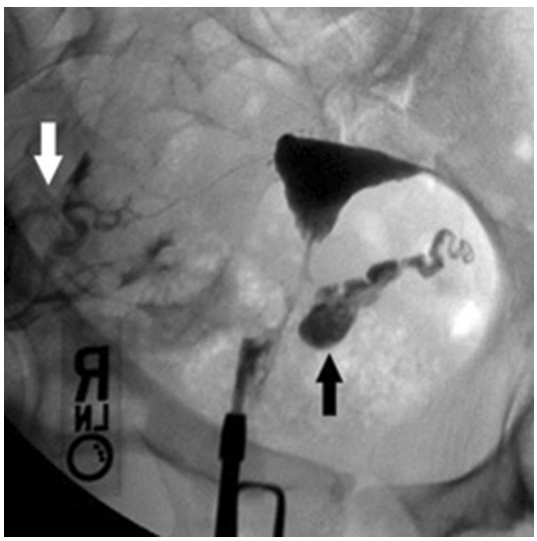

Fig. 2 Hydrosalpinx with peritubal adhesions. Hysterosalpingogram shows dilatation of the left fallopian tube with lack of free spillage from the distal tube (*black arrow*). Free spillage of contrast is noted from the right fallopian tube (*white arrow*)

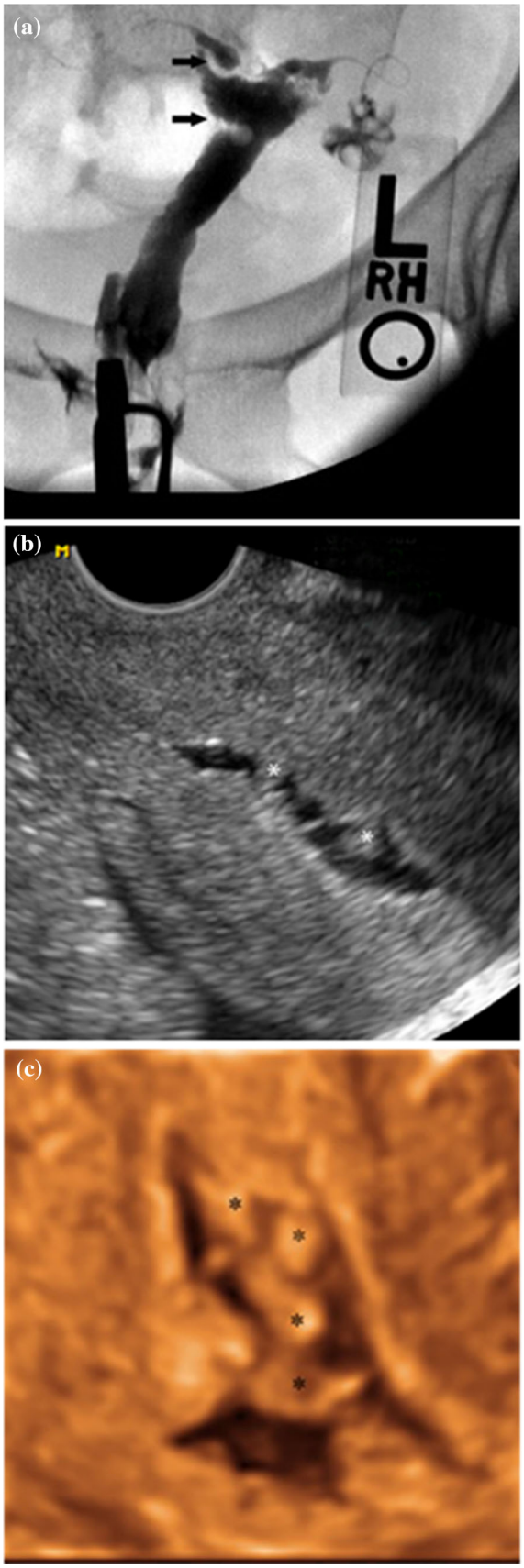

◀ **Fig. 3** **a** Asherman syndrome. Single image from a hysterosalpingogram shows diffuse narrowing of the endometrial cavity. Linear filling defects are likewise noted near the right cornu (*arrows*) that are consistent with intrauterine adhesions or synechiae. **b** Sonohysterogram shows poor distensibility of the endometrial cavity. The contour of the endometrial echo complex is diffusely irregular. Multiple echogenic nodules *asterisk* are noted within the endometrium that are consistent with intrauterine synechiae. **c** 3D sonohysterogram from same patient in **b** shows multiple nodular filling defects *asterisk* or synechiae within a diffusely irregular, poorly distensible endometrial cavity

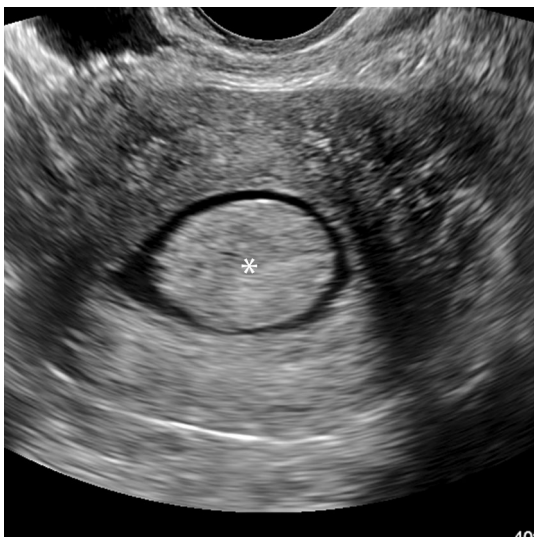

Fig. 4 Endometrial polyp. Sonohysterogram shows a sharply marginated, echogenic mass *asterisk* surrounded by fluid in the endometrial cavity

sonohysterography (SHSG) is considered the gold standard for the evaluation of the endometrium. SHSG can provide accurate detail regarding the size, shape, and number of endometrial masses [4]. The differential for intrauterine filling defects includes adhesions, polyps, and submucosal leiomyomas. Artifactual filling defects include air bubbles from injected contrast material and blood clots. Such filling defects are commonly transient and undergo positional change or spontaneously resolve as opposed to genuine endometrial filling defects.

Intrauterine adhesions or synechiae generally occur in the setting of prior pregnancy, aggressive dilatation and curettage, surgery, or infection [4]. Uterine synechiae can interfere with embryo transfer and implantation. Infertility secondary to uterine adhesions is known as Asherman syndrome. Imaging findings of synechiae include linear bands or filling defects with associated distortion or suboptimal distention of the endometrial cavity on conventional HSG or SHSG (Fig. 3a–c).

Endometrial polyps and submucosal fibroids may likewise interfere with successful embryonic implantation. Polyps are seen as ovoid intracavity filling defects at HSG or as focal thickening of the endometrial echo complex on pelvic US. Suspected polyps are best interrogated by SHSG

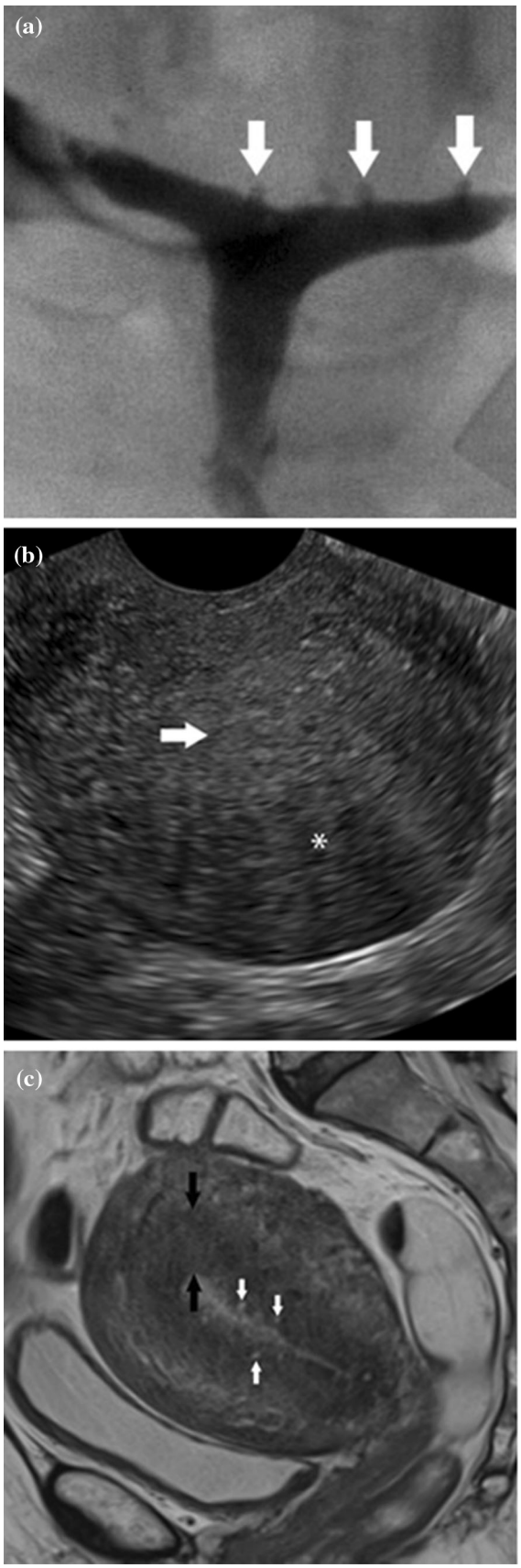

◀ **Fig. 5** **a** Adenomyosis. Hysterosalpingogram shows small contrast collections extending beyond the superior margin of the endometrial cavity. **b** Transvaginal ultrasound shows diffuse uterine enlargement with poor delineation between the myometrium *asterisk* and endometrium (*arrow*). **c** Sagittal T2-weighted MR shows diffuse, globular enlargement of the uterus with irregular thickening of the hypointense junctional zone (*black arrows*). Small hyperintense endometrial rests (*white arrows*) are likewise noted within the junction zone

which present as echogenic, intracavitary masses which may have cystic foci or a central vascular stalk on color Doppler interrogation [6] (Fig. 4).

Endometrial polyps are generally isoechoic to the background endometrium on ultrasound and are more centrally located in the endometrial cavity as opposed to submucosal fibroids. Most polyps may be readily resected by hysteroscopic polypectomy, whereas hysteroscopic resection of submucosal fibroids may only be feasible if greater than 50 % of the volume of the fibroid protrudes into the endometrial cavity [10]. Pregnancy rates following intrauterine insemination improved from 28 to 63 % following hysteroscopic polypectomy in one study [11].

Myometrial Disorders

Adenomyosis, leiomyomata, and Müllerian duct anomalies may be associated with infertility. While certain disorders of the myometrium may be suggested by conventional HSG as a focal contour abnormality, pelvic US provides far better evaluation with minimal cost, widespread availability, and lack of ionizing radiation. Pelvic MR is complimentary to US for the detection and characterization of myometrial disorders.

Adenomyosis is characterized by ectopic endometrial glandular tissue within the myometrium, with surrounding smooth-muscle hyperplasia [12]. Adenomyosis has been implicated in infertility due to impaired uterine contractility, leading to impaired sperm transport within the endometrial cavity [13]. There is a strong association between adenomyosis and pelvic endometriosis in women younger than 36 years, with adenomyosis being reported in approximately 90 % of these patients with endometriosis [13]. Adenomyosis may be diffuse or focal in the setting of an adenomyoma.

Adenomyosis may be suggested at HSG as linear or saccular contrast collections protruding from the endometrial cavity [4] (Fig. 5a). While US features of adenomyosis are often subtle, generally accepted findings include globular uterine enlargement, heterogeneous myometrial echotexture, indistinct uterine zonal anatomy, and asymmetric myometrial thickening [14] (Fig. 5b). However, the US sensitivity and specificity are still relatively low at 53–89 and 67–98 %, respectively [15].

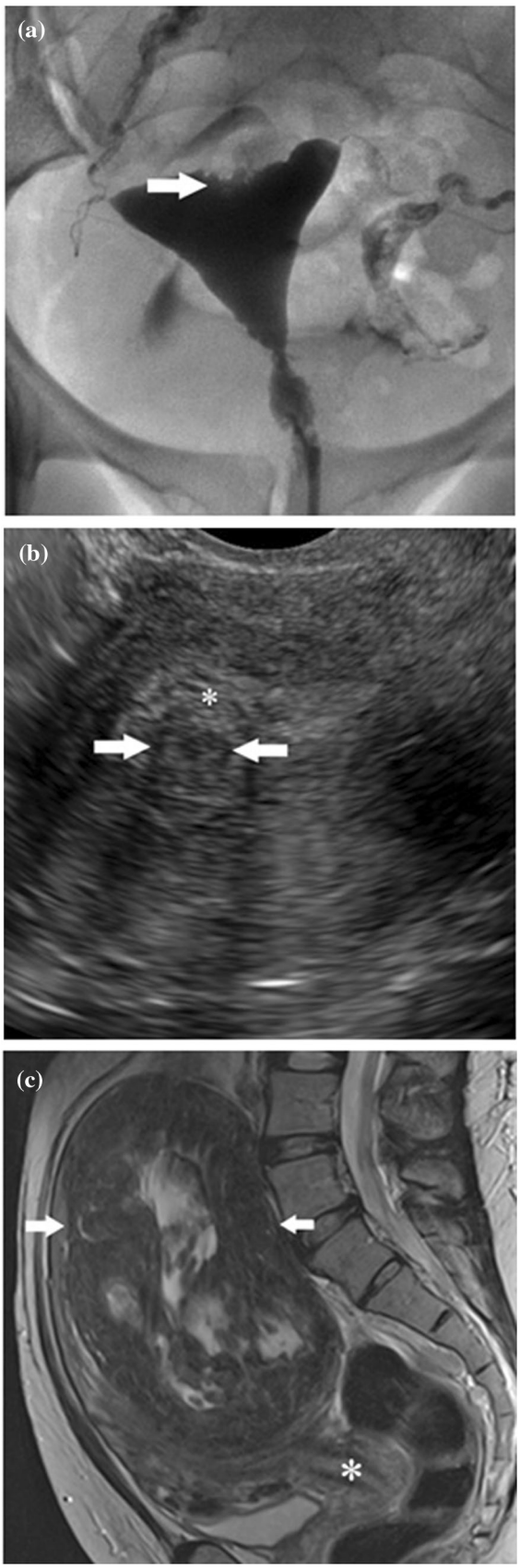

◀ **Fig. 6** **a** Submucosal leiomyoma. Hysterosalpingogram shows focal irregularity of the uterine contour along the fundal portion of the endometrium, consistent with a submucosal leiomyoma. **b** Transvaginal ultrasound from patient in **a** shows a hypoechoic mass (*white arrows*) indenting the adjacent endometrial echo complex *asterisk* consistent with a submucosal fibroid. **c** Sagittal T2-weighted MR shows a massive, sharply marginated, heterogeneous mass (*arrows*) arising from the lower uterine segment and cervix *asterisk* that essentially replaces the uterine corpus. Central hyperintensity within the mass is consistent with cystic degeneration

Pelvic MR remains the gold standard for the detection and characterization of adenomyosis, with reported sensitivity and specificity of 78–88 and 67–99 % [15], respectively. Findings include focal or diffuse thickening of the junctional zone greater than 12 mm. A junctional zone less than 8 mm virtually excludes adenomyosis, whereas a junctional zone between 8 and 12 mm can be equivocal and may require further investigation [4]. Additional MR findings include linear or nodular T1 and T2 hyperintense foci within the myometrium, representing ectopic endometrial rests [15] (Fig. 5c). The MR appearance of an adenomyoma is typically a poorly marginated myometrial mass that is hypointense on T1- and T2-weighted images.

Uterine leiomyomata or fibroids are the most common benign pelvic masses, as well as the most common cause of uterine enlargement in nonpregnant women [9]. Fibroids may be subserosal, intramural, or submucosal in location. Submucosal or intracavitary fibroids can interfere with embryo transfer and implantation. Gravid women with underlying fibroids have higher rates of malpresentation, preterm delivery, and spontaneous miscarriage [16].

At HSG, a fibroid may be suggested as an area of focal contour irregularity along the margin of the endometrial cavity, particularly if submucosal in location (Fig. 6a). Although rare, tubal occlusion can occur if the fibroid is near the cornu. Uterine fibroids are generally evident on pelvic US as sharply marginated, hypoechoic masses, although some less typical fibroids may be isoechoic or even hyperechoic relative to the background myometrium. While submucosal fibroids may be difficult to differentiate from endometrial polyps, they are generally hypoechoic relative to the endometrial echo complex, similar to myometrial echogenicity (Fig. 6b). Accurate differentiation between these two entities is crucial, since treatment options vary [17]. Diffuse uterine enlargement and heterogeneous echotexture can be seen in the setting of diffuse leiomyomatosis.

MR is considered the gold standard for optimal evaluation of the size, number, and anatomic location of suspected fibroids. MR is particularly valuable in establishing the exact relationship of the fibroid to the endometrial cavity. Uterine fibroids are readily evident on MR as sharply marginated myometrial masses that are generally

hypointense to the background myometrium on T2-weighted images and isointense to the myometrium on T1-weighted images. Less typically, fibroids may be iso- or even hyperintense on T2-weighted images in the setting of degeneration or cystic necrosis (Fig. 6c).

Müllerian Duct Anomalies

Congenital uterine anomalies, otherwise known as Müllerian duct anomalies, account for a significant percentage of infertile females. The reported prevalence varies significantly between 1 and 7 % [18]. Roughly 25 % of women with a Müllerian duct anomaly (MDA) experience reproductive problems, including increased rates of spontaneous abortion, prematurity, fetal growth restriction, abnormal fetal lie, and dystocia [19]. The prevalence of an MDA is three times higher in women with recurrent pregnancy loss [20].

The American Society of Reproductive Medicine system is the most commonly employed MDA classification scheme [21]. This system comprises seven classes (Table 1)

Although a complete description of Müllerian duct anomalies is well beyond the scope of this publication, accurate characterization of an MDA is essential, since pregnancy outcomes and treatment options vary for each anomaly[4]. Septate uterus is the most common variant, accounting for approximately 55 % of all MDAs and the reproductive outcome is the poorest, with a reported pregnancy loss rate of 65 % and preterm labor in 20 % of affected women [19].

MDAs may be initially detected at HSG as an unusual contour of the endometrial cavity (Fig. 7). However, HSG provides little to no detail regarding the myometrium and the external uterine contour, thereby limiting accurate evaluation.

US has a reported accuracy of 90–92 % for successful characterization and classification of MDAs, particularly with the employment of 3D techniques that provide superior visualization of the external uterine contour [22] (Fig. 8). As with other uterine disorders, MR remains the gold standard for the optimal evaluation of a suspected MDA with a reported accuracy approaching 100 % largely due to its excellent soft-tissue resolution and multiplanar imaging capabilities [23] (Fig. 9).

Table 1 Seven classes of Müllerian duct anomalies proposed by the American Society of Reproductive Medicine

Class I	Uterine hypoplasia and agenesis
Class II	Unicornuate uterus
Class III	Uterine didelphys
Class IV	Bicornuate uterus
Class V	Septate uterus
Class VI	Arcuate uterus
Class VII	Diethylstilbestrol (DES)-related anomalies

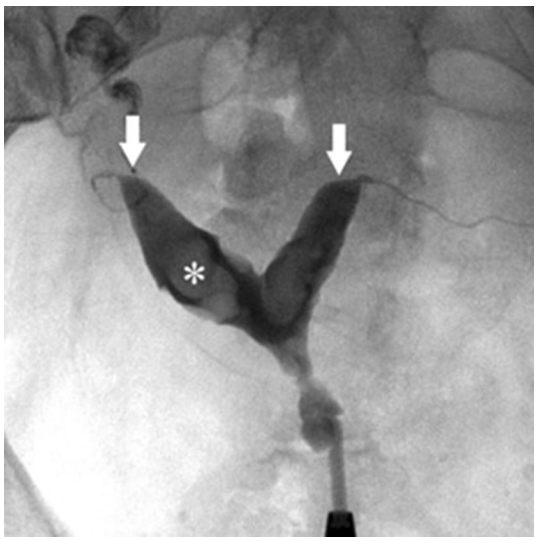

Fig. 7 Bicornuate uterus. Hysterosalpingogram shows widely divergent uterine horns that subsequently proved to represent a bicornuate uterus on a follow-up MRI. Multiple endometrial polyps *asterisk* were likewise incidentally seen

Fig. 8 Septate uterus. 3D ultrasound image shows divergent uterine horns (*black arrows*) separated by a muscular septum *asterisk*

Disorders of the Cervix

Cervical factor infertility is a condition in which an inadequate quality or quantity of cervical mucus is produced. The condition accounts for up to 10 % of cases of female infertility [4]. However, imaging plays no role in the evaluation of this disorder.

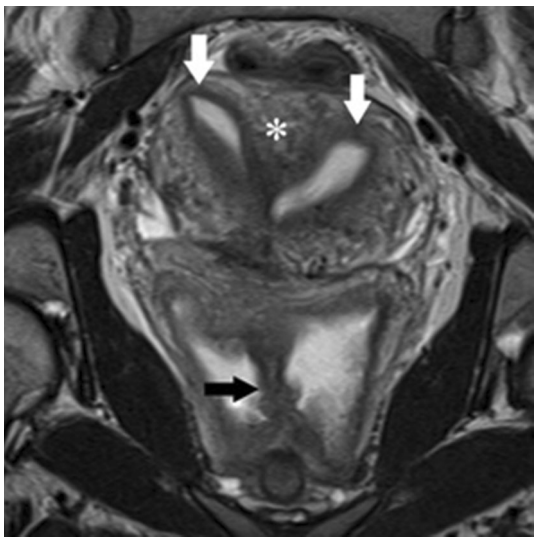

Fig. 9 Complete septate uterus. Oblique coronal T2-weighted MR shows two distinct uterine horns (*white arrows*) separated by a muscular septum *asterisk*. A prominent septum (*black arrow*) is likewise noted along the length of the vagina, consistent with a complete septate uterus

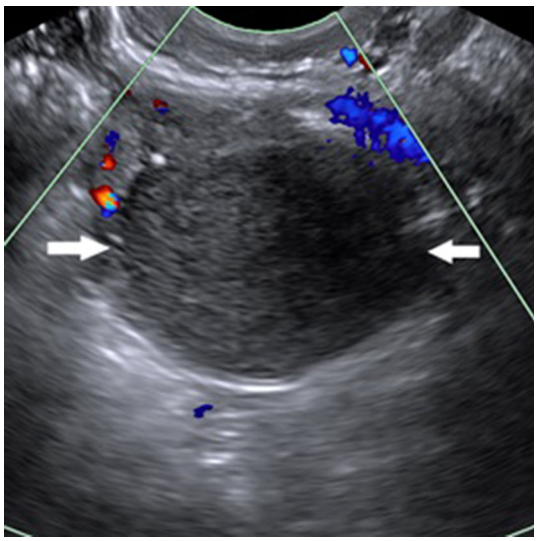

Fig. 10 Endometrioma. Transvaginal ultrasound shows a sharply marginated, homogeneous mass of intermediate echogenicity (*arrows*) that demonstrates no internal flow with color Doppler administration

Cervical stenosis is clinically defined as cervical narrowing that prevents the insertion of a 2.5-mm dilator [24]. It may be congenital or the result of prior infection or trauma, although cervical polyps, fibroids, and neoplasms may cause secondary cervical stenosis. Risk factors include previous cone biopsy, cryotherapy, and laser treatment [25]. It may lead to obstruction of menstrual flow, dysmenorrhea, or impaired fertility due to impaired sperm transit through the endocervical canal [24]. Although difficult to directly visualize, the inability to pass a catheter into the endometrial cavity at HSG usually confirms this condition. US-guided gradual dilation of the stenotic endocervical canal is commonly employed.

Disorders of the Peritoneum

Endometriosis is defined by the presence of extrauterine endometrial glands and stroma, generally within the peritoneal cavity [26]. The disorder occurs almost exclusively during reproductive years with symptoms ranging from none to debilitating pelvic pain. It is estimated that 30–50 % of affected women are infertile and that 20 % of infertile women have endometriosis [26]. Endometriosis may present as small pelvic implants or cysts that fluctuate in size and appearance throughout the menstrual cycle. The disease may also provoke an inflammatory response within the pelvis leading to fibrosis and pelvic adhesions [4].

Although HSG is relatively insensitive for the detection of endometriosis, loculated peritubal fluid collections may be seen from underlying adhesions due to endometriosis (Fig. 2). US features of endometriosis are variable. While US has a relatively low sensitivity for the detection of endometrial implants, discrete endometriomas are generally well visualized. The typical US appearance of an endometrioma is an adnexal mass with homogeneous, low-level internal echoes and hyperechoic mural foci that demonstrates no internal flow with Doppler interrogation [27] (Fig. 10).

While US is inherently insensitive to the presence of deeply infiltrating endometriosis (DIE), several investigators have recently described a transvaginal US technique to assess the mobility of pelvic structures, otherwise referred to as the "sliding sign." The transducer is placed in the posterior vaginal fornix to document the mobility or "sliding" of the uterus relative to the rectosigmoid colon while moving the transducer. A positive sliding sign is seen when the uterus and rectum move independently of one another, implying the absence of DIE. Conversely, a negative sliding sign suggests the presence of DIE in the cul-de-sac given the fixed or rigid appearance of the uterus relative to rectum. In a recent study, a negative sliding sign accurately predicted the presence of rectal DIE with a reported sensitivity and specificity of 85 and 96 %, respectively [28••].

The sensitivity and specificity for the detection of endometriosis on MR are considerably higher than US at 71 and 82 %, respectively [29]. The typical MR appearance of an endometrioma is an adnexal mass that is uniformly hyperintense on T1-weighted images and heterogeneous or decreased signal intensity on T2-weighted images, often referred to as "T2 shading" due to the variable chronicity of blood products within the

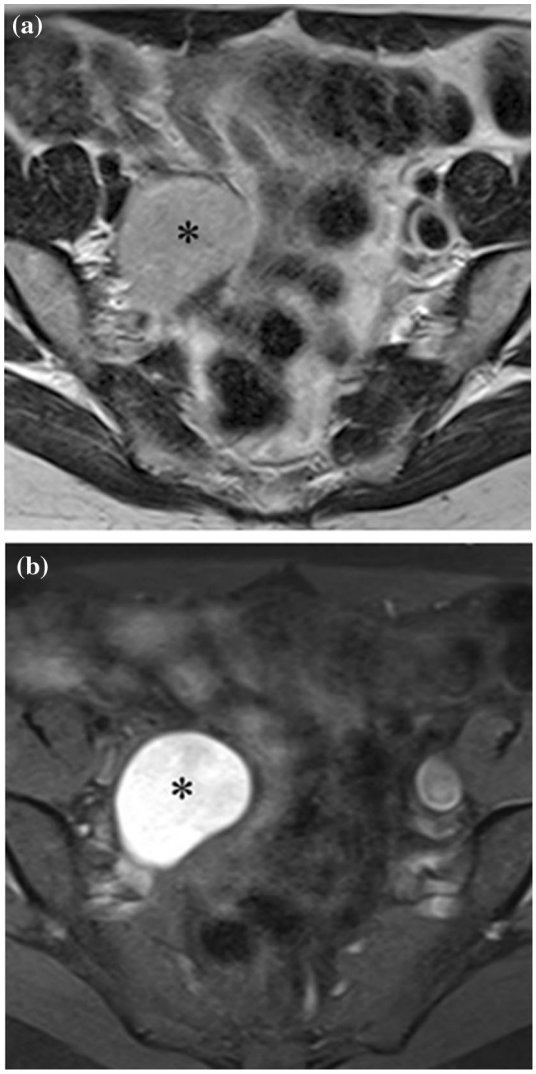

Fig. 11 **a** Endometrioma. Axial T2-weighted MR shows a well-circumscribed mass of intermediate signal intensity *asterisk* arising from the right ovary. **b** Axial T1-weighted MR with fat saturation from the same patient in **a** shows a markedly hyperintense mass arising from the right ovary

endometrioma [27] (Fig. 11a, b). Endometrial implants may be detected as small foci of increased signal intensity that are optimally detected on T1-weighted images with fat saturation. Endometriotic adhesions may be seen as amorphous, spiculated bands that are both T1 and T2 hypointense which commonly result in obliteration of organ interfaces and localized tethering or deformation of pelvic structures [30•] (Fig. 12).

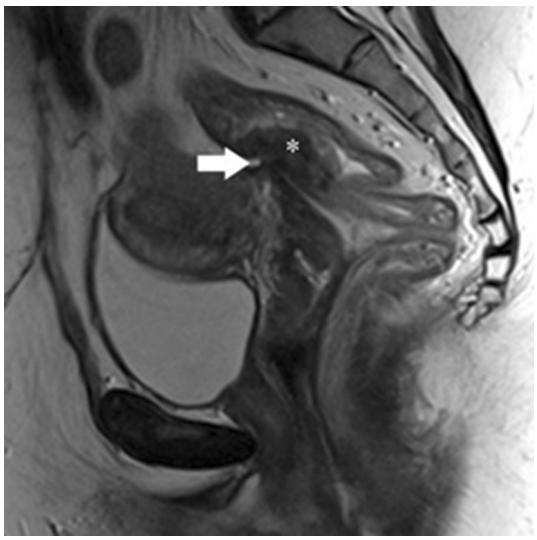

Fig. 12 Deeply infiltrating endometriosis. Sagittal T2-weighted MR shows a hypointense band (*arrow*) tethering the posterior margin of the lower uterine segment to the inferior margin of the distal sigmoid colon *asterisk*

Disorders of the Ovary

Primary ovarian disorders resulting in infertility are generally diagnosed on clinical and biochemical grounds and do not require imaging. Imaging is often essential for diagnosis of secondary abnormalities of the ovary, such as polycystic ovary syndrome (PCOS), endometriosis, and malignancy [4]. US is considered the primary imaging modality of choice for suspected ovarian disorders.

PCOS (also known as Stein–Leventhal syndrome) affects roughly 8 % of all women and is the most common endocrine disorder among women of reproductive age [31]. Specific clinical, biochemical, and radiological criteria must be met in order to establish the diagnosis. Furthermore, PCOS is a functional disorder; the morphologic features need not be present to establish the diagnosis, and conversely suggestive imaging findings do not establish the diagnosis in the absence of other signs and symptoms. Affected women demonstrate hyperandrogenism, which leads to morphologic changes in the ovary and elevated levels of luteinizing hormone [32]. Clinical manifestations include hirsutism, obesity, and oligomenorrhea.

US findings include bilateral ovarian enlargement, increased stromal echogenicity, and an increased number of small, peripherally located follicles [33] (Fig. 13a). An ovary containing 12 or more "cysts" was proved to be sensitive, but not specific for PCOS [9•]. The MR appearance of PCOS is that of symmetric, bilateral ovarian enlargement with peripheral, uniformly small, contiguous T2 hyperintense cysts [34] (Fig. 13b).

Male Infertility

A thorough history and physical examination of both partners may suggest a single or multifactorial etiology of infertility. In a multicenter study, the World Health

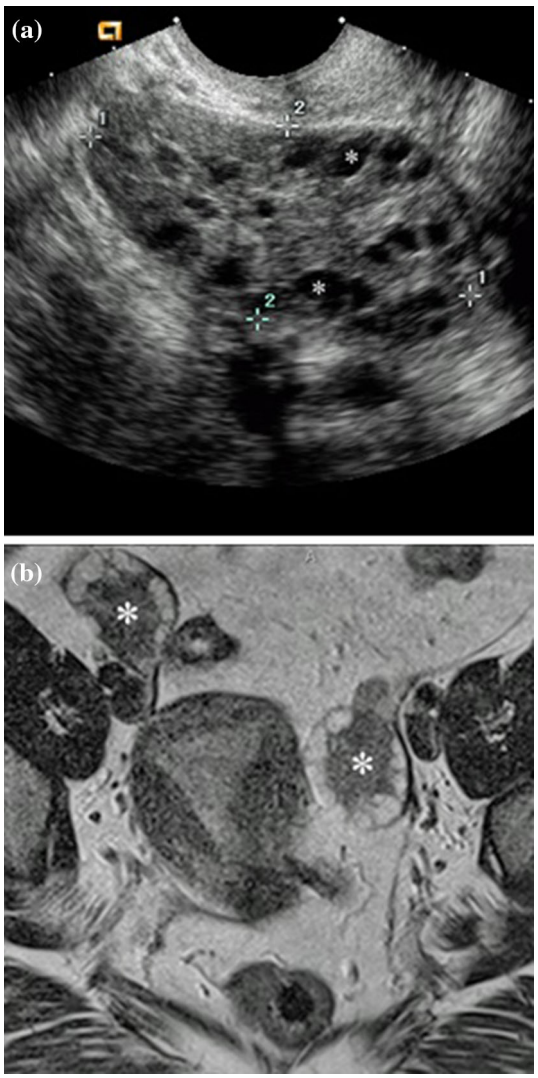

Fig. 13 **a** Polycystic ovarian syndrome. Transvaginal ultrasound shows diffuse enlargement of the right ovary with numerous, peripherally oriented follicles *asterisk*. **b** Coronal T2-weighted MR from patient in **a** shows bilateral ovarian enlargement *asterisk* with multiple, peripheral follicles in a contiguous or "string of beads" configuration

Organization found that 20 % of infertility cases were attributable to the male and that disorders in 27 % of infertile couples were attributable to both partners. Therefore, a male factor is present in approximately 50 % of cases [35]. After the diagnosis of male infertility has been established, a physical cause is identified in roughly 33 %, while the majority are classified as idiopathic [36].

US almost always serves as the primary imaging modality for the assessment of the infertile male due to its widespread availability, relatively low cost, and lack of ionizing radiation [36]. US can provide superb imaging of the scrotal structures, including the testes and epididymis. MRI of the scrotum is occasionally indicated as a problem-solving tool if US is inconclusive. Disorders of the male urogenital tract can be divided into three categories: pre-testicular, testicular, and post-testicular disorders.

Pre-testicular Disorders

Various abnormalities of the hypothalamic–pituitary–gonadal axis can result in male infertility [37]. Pre-testicular disorders include acquired or genetic endocrinopathies and disorders of the production or secretion of gonadotropin-releasing hormone, luteinizing hormone, or follicle-stimulating hormone. Most pre-testicular disorders do not require imaging. Rarely, a mass of the pituitary fossa may result in an alteration of luteinizing hormone or follicle-stimulating hormone levels that could adversely affect spermatogenesis.

Testicular Disorders

Imaging plays an important role in suspected primary disorders of the testes such as cryptorchidism, testicular atrophy, and varicocele. Less common conditions such as genetic disorders and gonadotoxin exposure do not require imaging.

Cryptorchidism is the failure of normal testicular descent into the scrotal sac and is the most common congenital abnormality of the male urogenital tract at birth [36]. Failure of testicular descent into the cooler environment of the scrotum is thought to impair spermatogenesis and is associated with a higher rate of primary testicular malignancy [38]. While fertility is generally not affected in the setting of unilateral cryptorchidism, infertility rates can be as high as 50 % in bilateral cryptorchidism [36]. While cryptorchidism may be suspected on physical exam, the diagnosis is readily established with US by the presence of a testis in the inguinal canal. CT or MR may occasionally be required if US is equivocal [39] (Fig. 14a, b).

Testicular atrophy can result in reduced spermatogenesis. Epididymo-orchitis is thought to cause testicular atrophy in spite of the lack of supporting epidemiological data [40]. The leading cause of epididymo-orchitis is sexually transmitted disease, usually from *Neisseria gonorrhea* and *Chlamydia trachomatis* [41]. Sexually transmitted epididymo-orchitis usually results in unilateral testicular atrophy. Less common etiologies include mumps and sarcoidosis, both of which are more insidious in onset and generally involve both testes. US findings in testicular atrophy include decreased volume, increased or heterogeneous testicular echogenicity, and decreased vascularity on color Doppler interrogation (Fig. 15).

A varicocele is an abnormal dilatation of the pampiniform plexus which may lead to impaired ipsilateral

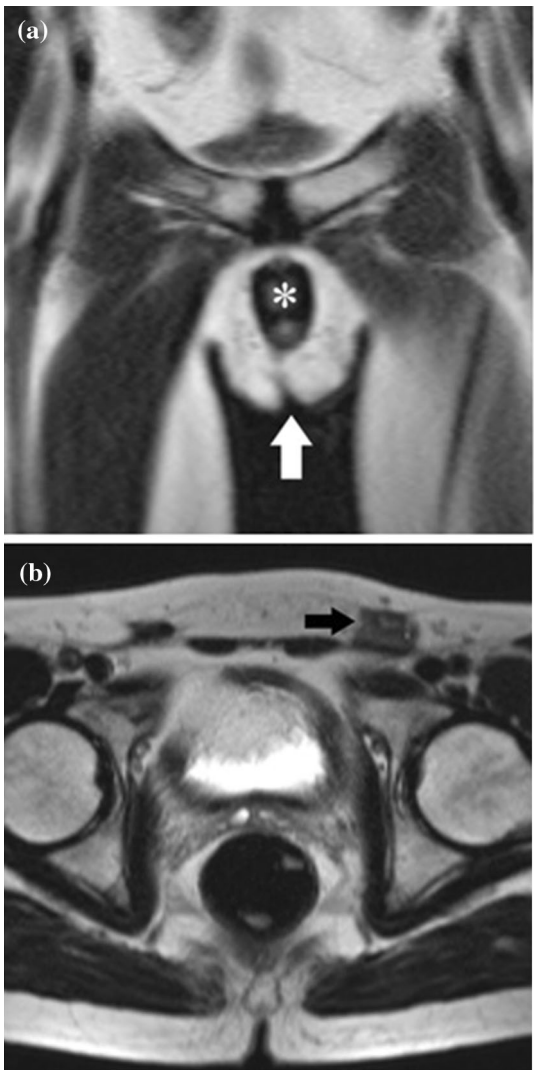

Fig. 14 **a** Cryptorchidism. Coronal T2-weighted MR shows an empty scrotal sac (*arrows*) immediately inferior to the penis *asterisk*. **b** Axial T2-weighted MR from the patient in **a** shows a hypointense mass in the left inguinal fossa, indicative of an atrophic, undescended testis. The right testis was not identified, presumably due to severe atrophy

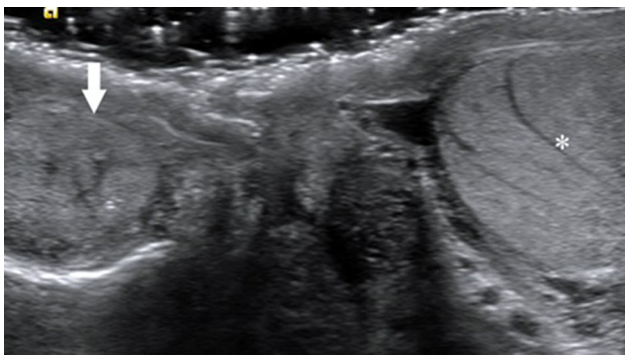

Fig. 15 Testicular atrophy. Transverse imaging from a scrotal ultrasound shows a diminutive, heterogeneous right testis (*arrow*) consistent with chronic atrophy. A normal sized left testis *asterisk* was noted

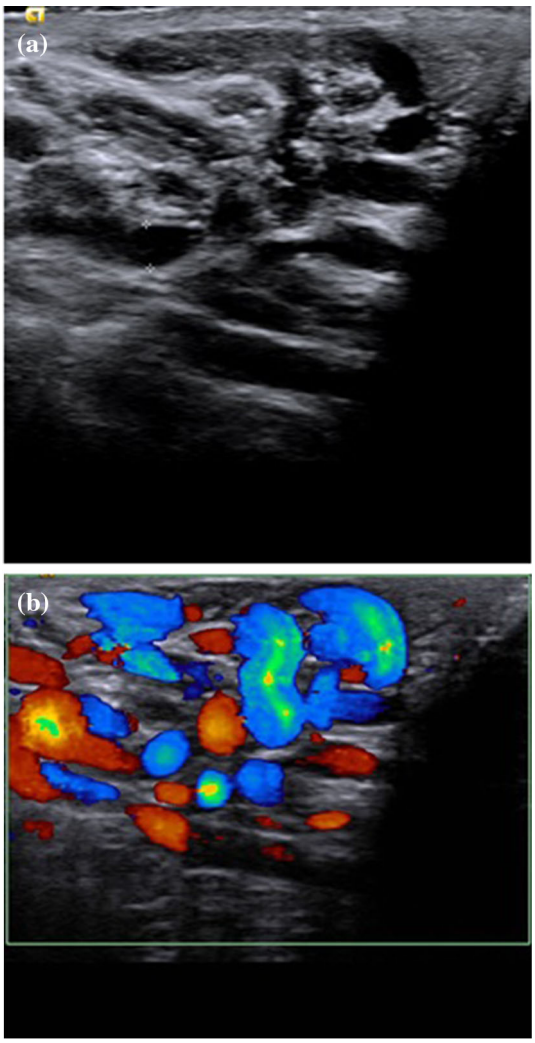

Fig. 16 **a** Varicocele. Grayscale US shows diffusely dilated veins of the left pampiniform plexus with the largest vessel measuring 4 mm. **b** Color Doppler image of the left hemi-scrotum in patient **a** demonstrates avid color flow throughout the pampiniform plexus in the setting of a varicocele

testicular growth and development with resultant impaired spermatogenesis [42]. Varicoceles are relatively common, and can be seen in 20 % of adolescents and adults and in up to 40 % of infertile males [43]. Symptoms include chronic pain, scrotal fullness, and discomfort. Although varicoceles are frequently detected on physical exam, US can confirm the diagnosis with a sensitivity of 97 % and specificity of 94 % [44]. Findings include prominent, serpiginous veins within the pampiniform plexus posterior to the testis, with at least 2–3 veins measuring <2–3 mm in diameter [36]. Color Doppler may demonstrate flow reversal on Valsalva maneuver which can improve diagnostic accuracy (Fig. 16a, b).

Fig. 17 Epididymal obstruction. Longitudinal image of the right scrotum shows diffusely dilated ductules of the epididymal head, presumably due to chronic epididymitis. The superior pole of the right testis *asterisk* is unremarkable

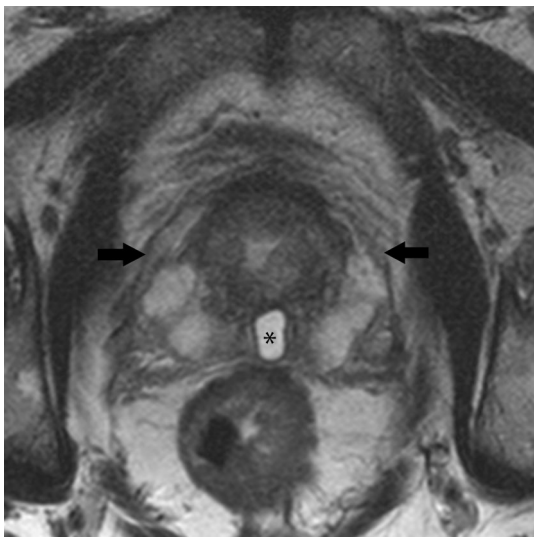

Fig. 18 Prostatic utricle. Axial T2-weighted image from a prostate MR shows a T2 hyperintense lesion *asterisk* within the posterior *midline* of the prostate (*arrows*)

Post-testicular Disorders

Post-testicular etiologies of infertility include disorders of erection and ejaculation, as well as immunologic disorders, none of which requires imaging. However, imaging plays an important role in suspected obstructive azoospermia (OA) or mechanical obstruction of the male reproductive tract. OA may occur anywhere along the course of the male reproductive tract, from testes to distal ductal system. US is considered the modality of choice for suspected OA, with up to 86 % of cases being detected by US in one recent study [45].

Obstruction at the level of the epididymis is often the result of prior epididymitis, usually due to gonococcal or chlamydial infection. Less common etiologies include iatrogenic injury from prior surgery. US findings include diffuse, serpiginous dilatation of the epididymis (Fig. 17). Vas deferens obstruction is generally the result of intentional occlusion in the setting of prior vasectomy. Concomitant epididymal dilatation is frequently seen in the setting of vas deferens obstruction. Less common etiologies include congenital absence of the vas deferens that is usually associated with cystic fibrosis [46].

Ejaculatory duct obstruction is a relatively rare condition that is either congenital or due to compression from an adjacent cystic midline lesion of the prostate, such as a utricle. Occlusion of the prostatic urethra is relatively uncommon and may be seen in the setting of either cystic dilatation of the prostatic urethra or prostatic periurethral cysts [36]. Although transrectal ultrasound is considered the modality of choice for suspected obstruction of the distal male reproductive tract, MR may provide better visualization of distal obstructive disorders due to its superior spatial resolution and multiplanar capability (Fig. 18).

Summary

The clinical evaluation of an infertile couple is a complex, multifactorial process that demands a systematic approach to both partners. Imaging plays an essential role in the workup of infertility in both genders. Clinical radiologists and reproductive medicine specialists must have a fundamental knowledge of both male and female genitourinary imaging to be effective members of the reproductive healthcare community. Additionally, practicing radiologists must have general understanding of the role of various imaging modalities employed for the assessment of infertility in both genders.

Compliance with Ethics Guidelines

Conflict of Interest Jeffrey Dee Olpin and Anne Kennedy each declare no potential conflicts of interest.

Human and Animal Rights and Informed Consent This article does not contain any studies with human or animal subjects performed by any of the authors.

References

Papers of particular interest, published recently, have been highlighted as:

• Of importance
•• Of major importance

1. Wright VC, Schieve LA, Reynolds MA, Jeng G, Kissin D. Assisted reproductive technology surveillance—United States, 2001. MMWR Surveill Summ. 2004;53(1):1–20.
2. McLaren JF. Infertility evaluation. Obstet Gynecol Clin N Am. 2012;39(4):453–63.
3. Chandra A, Martinez GM, Mosher WD, Abma JC, Jones J. Fertility, family planning, and reproductive health of U.S. women: data from the 2002 national survey of family growth. Vital Health Stat. 2005;25:1–160.
4. Steinkeler JA, Woodfield CA, Lazarus E, Hillstrom MM. Female infertility: a systematic approach to radiologic imaging and diagnosis. Radiographics. 2009;29(5):1353–70.
5. Imaoka I, Wada A, Matsuo M, Yoshida M, Kitagaki H, Sugimura K. MR imaging of disorders associated with female infertility: use in diagnosis, treatment, and management. Radiographics. 2003;23(6):1401–21.
6. Simpson WL Jr, Beitia LG, Mester J. Hysterosalpingography: a reemerging study. Radiographics. 2006;26(2):419–31.
7. Krysiewicz S. Infertility in women: diagnostic evaluation with hysterosalpingography and other imaging techniques. Am J Roentgenol. 1992;159(2):253–61.
8. Thurmond AS. Imaging of female infertility. Radiol Clin N Am. 2003;41(4):757–67.
9. • Sadow CA, Sahni VA. Imaging female infertility. Abdom Imaging. 2014;39(1):92–107. *While the diagnostic criteria for polycystic ovarian disease can vary, clearcut guidelines for this diagnosis is outlined in this article.*
10. Lev-Toaff AS, Toaff ME, Liu JB, Merton DA, Goldberg BB. Value of sonohysterography in the diagnosis and management of abnormal uterine bleeding. Radiology. 1996;201(1):179–84.
11. Perez-Medina T, Bajo-Arenas J, Salazar F, Redondo T, Sanfrutos L, Alvarez P, et al. Endometrial polyps and their implication in the pregnancy rates of patients undergoing intrauterine insemination: a prospective, randomized study. Hum Reprod. 2005;20(6):1632–5.
12. Matalliotakis IM, Katsikis IK, Panidis DK. Adenomyosis: what is the impact on fertility? Curr Opin Obstet Gynecol. 2005;17(3):261–4.
13. Kunz G, Beil D, Huppert P, Noe M, Kissler S, Leyendecker G. Adenomyosis in endometriosis–prevalence and impact on fertility. Evidence from magnetic resonance imaging. Hum Reprod. 2005;20(8):2309–16.
14. Atri M, Reinhold C, Mehio AR, Chapman WB, Bret PM. Adenomyosis: US features with histologic correlation in an in vitro study. Radiology. 2000;215(3):783–90.
15. Tamai K, Togashi K, Ito T, Morisawa N, Fujiwara T, Koyama T. MR imaging findings of adenomyosis: correlation with histopathologic features and diagnostic pitfalls. Radiographics. 2005;25(1):21–40.
16. Klatsky PC, Tran ND, Caughey AB, Fujimoto VY. Fibroids and reproductive outcomes: a systematic literature review from conception to delivery. Am J Obstet Gynecol. 2008;198(4):357–66.
17. Somigliana E, Vercellini P, Daguati R, Pasin R, De Giorgi O, Crosignani PG. Fibroids and female reproduction: a critical analysis of the evidence. Hum Reprod Update. 2007;13(5):465–76.
18. Saravelos SH, Cocksedge KA, Li TC. Prevalence and diagnosis of congenital uterine anomalies in women with reproductive failure: a critical appraisal. Hum Reprod Update. 2008;14(5):415–29.
19. Troiano RN, McCarthy SM. Mullerian duct anomalies: imaging and clinical issues. Radiology. 2004;233(1):19–34.
20. Grimbizis GF, Camus M, Tarlatzis BC, Bontis JN, Devroey P. Clinical implications of uterine malformations and hysteroscopic treatment results. Hum Reprod Update. 2001;7(2):161–74.
21. The American fertility society classifications of adnexal adhesions, distal tubal occlusion, tubal occlusion secondary to tubal ligation, tubal pregnancies, mullerian anomalies and intrauterine adhesions. *Fertil Steril*. 1988;49(6):944–55.
22. Pellerito JS, McCarthy SM, Doyle MB, Glickman MG, DeCherney AH. Diagnosis of uterine anomalies: relative accuracy of MR imaging, endovaginal sonography, and hysterosalpingography. Radiology. 1992;183(3):795–800.
23. Mueller GC, Hussain HK, Smith YR, Quint EH, Carlos RC, Johnson TD, et al. Mullerian duct anomalies: comparison of MRI diagnosis and clinical diagnosis. Am J Roentgenol. 2007;189(6):1294–302.
24. Baldauf JJ, Dreyfus M, Wertz JP, Cuenin C, Ritter J, Philippe E. Consequences and treatment of cervical stenoses after laser conization or loop electrosurgical excision. J Gynecol Obstet Biol Reprod. 1997;26(1):64–70.
25. Christianson MS, Barker MA, Lindheim SR. Overcoming the challenging cervix: techniques to access the uterine cavity. J Low Genit Tract Dis. 2008;12(1):24–31.
26. Eskenazi B, Warner ML. Epidemiology of endometriosis. Obstet Gynecol Clin N Am. 1997;24(2):235–58.
27. Woodward PJ, Sohaey R, Mezzetti TP Jr. Endometriosis: radiologic-pathologic correlation. Radiographics. 2001;21(1):193–216.
28. •• Hudelist G, Fritzer N, Staettner S, Tammaa A, Tinelli A, Sparic R, et al. Uterine sliding sign: a simple sonographic predictor for presence of deep infiltrating endometriosis of the rectum. *Ultrasound Obstet Gynecol*. 2013;41(6):692–5. *The sliding sign is an important, recently described technique that provides a quick and cost effective evaluation for uterorectal adhesions in the setting of diffusely infiltrating endometriosis.*
29. Zawin M, McCarthy S, Scoutt L, Comite F. Endometriosis: appearance and detection at MR imaging. Radiology. 1989;171(3):693–6.
30. • Macario S, Chassang M, Novellas S, Baudin G, Delotte J, Toullalan O, et al. The value of pelvic MRI in the diagnosis of posterior cul-de-sac obliteration in cases of deep pelvic endometriosis. *Am J Roentgenol*. 2012;199(6):1410–5. *The study provides invaluable current insight into the challenging MR diagnosis of deeply infiltrating endometriosis.*
31. Teede H, Deeks A, Moran L. Polycystic ovary syndrome: a complex condition with psychological, reproductive and metabolic manifestations that impacts on health across the lifespan. BMC Med. 2010;8:41.
32. Legro RS, Barnhart HX, Schlaff WD, Carr BR, Diamond MP, Carson SA, et al. Clomiphene, metformin, or both for infertility in the polycystic ovary syndrome. N Engl J Med. 2007;356(6):551–66.
33. Pache TD, Wladimiroff JW, Hop WC, Fauser BC. How to discriminate between normal and polycystic ovaries: transvaginal US study. Radiology. 1992;183(2):421–3.
34. Kimura I, Togashi K, Kawakami S, Nakano Y, Takakura K, Mori T, et al. Polycystic ovaries: implications of diagnosis with MR imaging. Radiology. 1996;201(2):549–52.
35. Jose-Miller AB, Boyden JW, Frey KA. Infertility. Am Fam Physician. 2007;75(6):849–56.
36. Ammar T, Sidhu PS, Wilkins CJ. Male infertility: the role of imaging in diagnosis and management. Br J Radiol. 2012;85:S59–68.
37. Brugh VM 3rd, Lipshultz LI. Male factor infertility: evaluation and management. Med Clin N Am. 2004;88(2):367–85.

38. Kurpisz M, Havryluk A, Nakonechnyj A, Chopyak V, Kamieniczna M. Cryptorchidism and long-term consequences. Reprod Biol. 2010;10(1):19–35.
39. Dogra VS, Gottlieb RH, Oka M, Rubens DJ. Sonography of the scrotum. Radiology. 2003;227(1):18–36.
40. Schuppe HC, Pilatz A, Hossain H, Meinhardt A, Bergmann M, Haidl G, et al. Orchitis and male infertility. Urol A. 2010;49(5):629–35.
41. Stewart VR, Sidhu PS. The testis: the unusual, the rare and the bizarre. Clin Radiol. 2007;62(4):289–302.
42. Beddy P, Geoghegan T, Browne RF, Torreggiani WC. Testicular varicoceles. Clin Radiol. 2005;60(12):1248–55.
43. Weidner W, Pilatz A, Altinkilic B. Andrology: varicocele: an update. Urol A. 2010;49(Suppl 1):163–5.
44. Trum JW, Gubler FM, Laan R, van der Veen F. The value of palpation, varicoscreen contact thermography and colour Doppler ultrasound in the diagnosis of varicocele. Hum Reprod. 1996;11(6):1232–5.
45. Moon MH, Kim SH, Cho JY, Seo JT, Chun YK. Scrotal US for evaluation of infertile men with azoospermia. Radiology. 2006;239(1):168–73.
46. Donat R, McNeill AS, Fitzpatrick DR, Hargreave TB. The incidence of cystic fibrosis gene mutations in patients with congenital bilateral absence of the vas deferens in Scotland. Br J Urol. 1997;79(1):74–7.